Environmental Science: Atmospheres

ROYAL SOCIETY OF CHEMISTRY

PAPER

View Article Online
View Journal | View Issue

Cite this: *Environ. Sci.: Atmos.*, 2021, **1**, 176

Mineral and biological ice-nucleating particles above the South East of the British Isles†

A. Sanchez-Marroquin, *[a] J. S. West, [b] I. T. Burke,[a] J. B. McQuaid [a] and B. J. Murray [a]

A small fraction of aerosol particles known as Ice-Nucleating Particles (INPs) have the potential to trigger ice formation in cloud droplets at higher temperatures than homogeneous freezing. INPs can strongly reduce the water content and albedo of shallow mixed-phase clouds and also influence the development of convective clouds. Therefore, it is important to understand which aerosol types serve as INPs and how effectively they nucleate ice. Using a combination of INP measurements and Scanning Electron Microscopy with Energy Dispersive Spectroscopy (SEM-EDS), we quantify both the INP concentrations over a range of activation temperatures and the size-resolved composition. We show that the INP population of aerosol samples collected from an aircraft over the UK during July of 2017 is consistent with ice-nucleation on mineral dust below about −20 °C, but some other INP type must account for ice-nucleation at higher temperatures. Biological aerosol particles above ~2 μm were detected based on visual detection of their morphological features in all the analysed samples at concentrations of at least 10 to 100 L^{-1} in the boundary layer. We suggest that given the presence of biological material, it could substantially contribute to the enhanced ice-nucleation ability of the samples at above −20 °C. Organic material attached to mineral dust could be responsible for at least part of this enhancement. These results are consistent with a growing body of data which suggests mineral dust alone cannot explain the INP population in the mid-latitude terrestrial atmosphere and that biological ice nucleating particles are most likely important for cloud glaciation.

Received 8th January 2021
Accepted 25th March 2021

DOI: 10.1039/d1ea00003a

rsc.li/esatmospheres

Environmental significance

The formation of ice in clouds strongly influences their properties and their role in climate. However, our knowledge of which aerosol particles serve as Ice-Nucleating Particles (INP) and their concentration in the atmosphere is poorly defined; this is especially so at altitudes requiring an airborne platform. To help address this problem we collected aerosol samples using an aircraft around the South East of the British Isles and then measured INP concentrations and aerosol composition offline. The results indicate that mineral dust alone cannot account for the observed INPs. We suggest that this important additional type of INPs is very likely of biological origin.

1 Introduction

The lifetime, precipitation and radiative properties of clouds that contain both supercooled water and ice (mixed-phase clouds) are significantly affected by the presence of aerosol particles that can trigger ice formation.[1–3] These particles are known as Ice-Nucleating Particles (INPs). Climate models tend to oversimplify and poorly represent the ice-related processes such as ice formation triggered by the presence of INPs. INPs and ice production are important in deep convective clouds,[4,5] as well as shallow clouds,[3] but it is becoming increasingly clear that the representation of ice-processes is particularly important in defining the amount of water and ice that models produce in shallow clouds.[6–8] This difficulty in properly representing the amount of supercooled water in shallow mid- and high-latitude mixed-phase clouds is a key cause of the large uncertainty in the negative cloud-phase feedback.[9,10] This feedback is produced by the fact that as the atmosphere warms, water will replace ice in mixed-phase clouds, increasing their albedo. The strength of this feedback depends on how much supercooled water and ice there is present day clouds.[11]

Given that INPs are important for defining the cloud phase feedback, it is therefore very important to characterise the sources of INPs to properly represent the ice-related processes in climate models. Mineral dust from the deserts is known to be one of the most relevant sources of INPs worldwide, both

[a]School of Earth and Environment, University of Leeds, Woodhouse Lane, Leeds, LS2 9JT, UK. E-mail: a.sanchezmarroquin@leeds.ac.uk; b.j.murray@leeds.ac.uk
[b]Biointeractions and Crop Protection Dept., Rothamsted Research, Harpenden, AL5 2JQ, UK

† Electronic supplementary information (ESI) available. See DOI: 10.1039/d1ea00003a

because of its abundance throughout the atmosphere and its relatively high ice-nucleation ability below −15 °C.[12–15] Although most of the dust present in the atmosphere is emitted from hot and arid deserts,[16] significant amounts of dust are emitted from anthropogenic activities such as agriculture (which could contribute up to ∼25% of the global burden[17]) or from high-latitude dust sources.[18] Ash from volcanic eruptions, which has some similarities to desert dust in composition, has also been identified as a source of INPs.[19–22] Other known sources of INPs are sea-spray aerosol containing marine organic material,[23–26] biological aerosol particles from terrestrial locations such as pollen, bacteria or fungal fragments.[27–29] Additionally, ice-nucleation macromolecules of biological origin can become attached to mineral or soil dust particles.[30–33] Fertile soil dust generally has a higher ice-nucleation ability than desert dusts, due to the biological material which is internally mixed with the dust particles.[34–36] However, the relative contribution of biological INPs compared to the contribution of mineral dust at altitudes where mixed-phase clouds can occur in mid- to high-latitudes has not been fully addressed. This question is particularly relevant since the majority of the measurements of biological INPs are carried out at ground level. In different modelling studies, sea-spray aerosol containing marine organic material has been found to compete with mineral dust at altitudes where mixed-phase clouds can occur, particularly in remote oceans.[14,37,38] However, it is not clear if terrestrial sources of biological INPs could compete with mineral dust at cloud relevant altitudes.[39–43]

The freezing temperatures of biological INPs tend to be higher than those for mineral dust INPs.[1,44] Similar behaviour is observed in many atmospheric INP measurements,[45,46] where biological material is commonly responsible for the ice-nucleation properties of an aerosol sample in the higher end of its temperature spectrum, while dust tends to be the dominant INP type at temperatures below ∼−20 °C. Although surface measurements show that there is a significant biogenic component to the INP population,[45–47] these measurements might have been influenced by the proximity to these sources of INPs. Hence, measurements at altitude are necessary to see if the INP population across the boundary are also enhanced above mineral dust. In spite of the technical and logistical difficulties of measuring INPs on board of aircraft, this has been done in different locations including the Arctic,[48–51] North America,[52] the Pacific,[53,54] the Tropical Atlantic,[55] Iceland,[56] or the Eastern Mediterranean.[57] However, aircraft measurements of INPs have never been conducted above the UK.

Here, we present a dataset of INP concentration measurements alongside the aerosol size-resolved composition obtained using Scanning Electron Microscopy with Energy Dispersive Spectroscopy (SEM-EDS) of aerosol samples collected in the south of the UK during July 2017. In order to avoid potential biases from the aerosol emitted at the ground level, we collected aerosol particles at different altitudes within the boundary layer. The data obtained from these techniques are used to estimate the contribution of mineral dust to the INP population.

2 Experimental

2.1 Sampling platform

The aerosol samples shown here have been collected on board of the FAAM BAe-146. This research aircraft has a wide range of instruments to measure different atmospheric properties. Here we have collected aerosol particles on top of filters for offline analysis using the filter inlet system on board of the FAAM BAe-146. Most of the aerosol samples have been acquired opportunistically during research flights that were carried out within the Effect of Megacities on the transport and transformation of pollutants on the Regional and Global scale (EMeRGe) campaign, in July 2017, close to the city of London. Samples from an Oil and Gas research flight on the 11th of July 2017 as well as a FAAM test flight on the 27th of September 2017 are also shown.

The analysis of our filter samples has been complemented with data from different instruments. The Passive Cavity Aerosol Spectrometer probe 100-X (PCASP) and the Cloud Droplet Probe (CDP) are underwing optical particle counters, which have been used to measure the size distribution of the aerosol particles.[58] These instruments measure the optical diameters of aerosol particles in an approximated range of 0.1 to 3 μm and 2 to 50 μm respectively. O_3 and CO measurements from the TE49C UV Photometric Ozone analyser by Thermo Scientific and AL5002 Fast Fluorescence CO Analyser by Aerolaser GmbH instruments respectively were also used. Other measurements that have been used in the present study are the pressure altitude and aircraft location. Our sampling strategy systematically involves avoiding sampling in cloudy conditions. The inlet line was closed immediately whenever we had online indication of the presence of liquid water or ice (detected using the CDP). The dew point temperature was monitored, being always at least a few degrees below the true air temperature. All the complementary data was downloaded *via* the Centre for Environmental Data Analysis (CEDA).

2.2 Aerosol particle sampling

Aerosol particles have been collected on top of filters using the filter inlet system on board of the FAAM BAe-146. This filter inlet system has been previously used for aerosol collection.[55,56,59–62] This system and the used set up has been described and characterised previously.[63] The system has a bypass that can be used to regulate the flow and minimise the sub-isokinetic enhancement, it was operated with this bypass fully open. This filter inlet system can sample particles smaller than ∼20 μm on top of two filters simultaneously. Most of the samples have been collected on top of a polycarbonate with a pore size of 0.4 μm and a Teflon filter with an equivalent pore size of 0.45 μm simultaneously. Polycarbonate filters have been analysed using SEM-EDS at the University of Leeds in order to characterise their size-resolved composition, while Teflon filters have been used to quantify the INP concentration using a droplet-based assay.

Most samples were taken in the South-East of the UK, as shown In Fig. 1a, where the flight tracks corresponding to the sampling locations are displayed. Further information

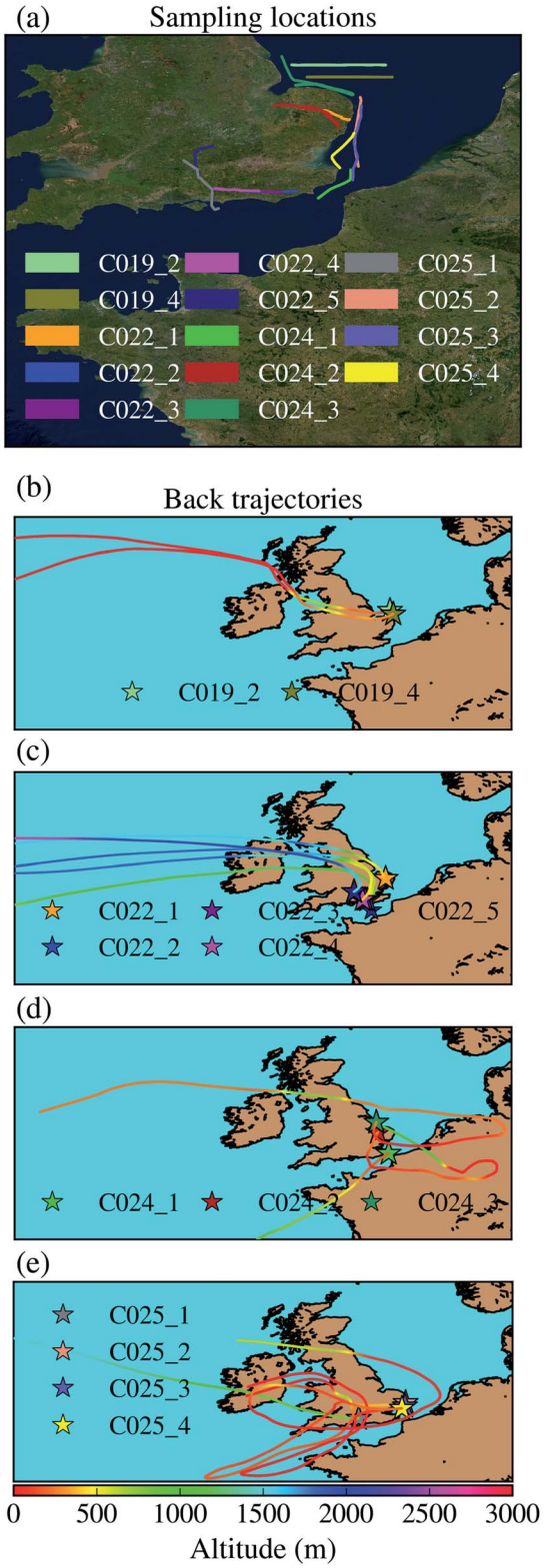

Fig. 1 (a) Flight tracks of the sampling locations. (b–e) HYSPLIT analysis of the 4 day back trajectories of the air masses where the samples were taken. Each of the panels contains the samples collected in each of the four days of the campaign. The back trajectory associated with each air mass has been coloured based on its altitude. The stars correspond to the starting point of each back trajectory, which is the middle point of the sampling location.

corresponding to these samples can be found in Table 1. In order to investigate the origin of the air masses where the samples were collected, we ran Hybrid Single-Particle Lagrangian Integrated Trajectory (HYSPLIT) back trajectories using a Python package described in a previous study.[64] The air parcel trajectories were calculated using the Global Data Assimilation System 3 hour meteorology reanalysis product. Back trajectories were run from an approximated middle point in between the starting and the ending sampling time. This analysis is shown in Fig. 1b. As shown, all samples apart from one were collected in the boundary layer.

2.3 Ice-nucleating particle measurements

INPs have been measured using a filter droplet-on-filter assay that has been previously used during other FAAM BAe-146 field campaigns.[55,56] This technique is a combination of the techniques used in previous studies.[53,65] Teflon filters where aerosol samples have been collected using the filter inlet system on board of the FAAM BAe-146 are placed on top of glass slides (Ted Pella cover glass, 48 × 60 × 0.15 mm), whose surface was made hydrophobic by applying Turtle Wax ClearVue Rain repellent solution. The glass slides are placed on top of a cold stage over a thin layer of silicone oil to improve the thermal contact. About 60 pure water (Milli-Q®) droplets of 2 μL are pipetted on top of the exposed filters. The system is cooled at a constant rate of 1 K min^{-1} while a camera records the freezing of the droplets at the same time as stage temperature measurements are automatically taken. This allows us to obtain the fraction of droplets frozen as a function of temperature, $ff(T)$. In order to prevent condensation and frost growth, the experiment is performed in a chamber that is flushed using a ~0.2 L min^{-1} flow of dry nitrogen (zero grade). The $ff(T)$ calculated using this experiment is shown in Fig. 2a. The INP concentrations, which have been calculated from $f(T)$ using the eqn (1), are shown in Fig. 2b.

$$[\mathrm{INP}](T) = -\ln(1 - ff(T))\frac{A_{\mathrm{fil}}}{V_{\mathrm{a}}\alpha} \quad (1)$$

where $A_{\mathrm{fil}} = 11$ cm^2 is the exposed area of the filter, V_{a} is the sampled air volume, and $\alpha = 1.375$ cm^2 is the contact surface of each droplet. The contact surface has been calculated from a droplet contact angle of 126°, assuming spherical cap geometry. The errors have been calculated using the same Monte Carlo algorithm as in ref. 56. This error includes the uncertainty associated with the randomness of the distribution of freezing sites within the experiment, as well as a range of contact angles from ~110 to ~130°. These calculations are based on the singular description of the ice-nucleation phenomenon. Although ice-nucleation is a stochastic process, this description assumes that the time-dependence is of second order in comparison with the distribution of the ice-nuclei types through the droplets.[1] This approach has been extensively used for many years in different laboratory, fieldwork and modelling studies. However, in the analysis it is usually assumed that the surface area of the aerosol particles is homogenously scattered through the droplet population. Hence, large variability in the surface area of the aerosol

Table 1 Summary of the samples collected for this study. The symbol * indicates that there was at least one manual sampling interruption during the collection in order to avoid sampling during a change in the altitude or an abrupt turn. Teflon position indicates in which of the identical lines of the filter inlet system (up or low[63]) the Teflon filter has been used. Therefore, the polycarbonate filter has been collected in the other line. The given value of dust surface area is calculated by integrating the mineral dust surface area (total surface area multiplied by the fraction of particles in the categories Si rich, Si only, Al–Si rich and Ca rich in each bin). The number in the bracket after the dust surface area corresponds to the error of the magnitude calculated using Poisson counting statistics. Samples where there is not a value for the surface area of the mineral dust were not be analysed using SEM-EDS. In the last column, samples have been labelled according to the sampling location and air mass origin. O&G corresponds to the samples collected during the Oil and Gas flight. Downwind and upwind (of London) correspond to the samples collected within the boundary layer close to London. Continental Europe refers to the samples collected on the C024 flight, whose air masses have a higher influence from continental Europe. The C022_5 sample has been collected above the boundary layer

Sample	Date (2017)	Start time	End time	Pressure altitude (m)	Radar altitude (m)	Vol. PC (L)	Vol. tef. (L)	Teflon position	Dust area (μm^2 cm^{-3})	% dust area	Description
C019_2	07/11th	10:06	10:24	185	154	438	—	—	2.9 (1.1)	17	O&G
C019_4	07/11th	11:19	19:37	330	303	286	160	Up	—	—	O&G
C022_1	07/17th	09:29	09:41*	220	303	182	110	Up	9.8 (3.5)	28	Upwind
C022_2	07/17th	10:23	10:39	648	714	335	149	Low	—	—	Downwind
C022_3	07/17th	10:48	11:03	478	534	335	255	Up	—	—	Downwind
C022_4	07/17th	11:10	11:18	331	392	286	84	Low	—	—	Downwind
C022_5	07/17th	11:58	12:10	1450	1490	258	—	Up	2.9 (1.4)	33	Above boundary layer
C024_1	07/19th	12:59	13:10	202	160	171	97	Up	—	—	Continental Europe
C024_2	07/19th	13:28	14:03*	351	250	696	257	Low	31.0 (5.7)	45	Continental Europe
C024_3	07/19th	15:20	15:51	347	281	953	250	Up	14.6 (1.7)	35	Continental Europe
C025_1	07/20th	12:51	13:09	943	837	425	189	Low	10.9 (2.9)	41	Upwind
C025_2	07/20th	13:40	14:03*	364	301	672	195	Up	5.1 (1.2)	38	Downwind
C025_3	07/20th	14:11	14:35	76	38	625	260	Low	11.9 (2.8)	37	Downwind
C025_4	07/20th	14:41	14:54	182	153	218	122	Up	—	31	Downwind

per droplet can lead to significant biases when calculating magnitudes such as the INP concentration using droplet-based assays.[66] In the Sect. S1,† we use Monte Carlo simulations to show the distribution of surface area through the droplet populations of our experiments for one of our samples. Our analysis suggests that 95% of the droplets have a supermicron surface area within ~4% of the mean. Hence, we consider that the assumption of a constant surface area per droplet is justified.

Some samples were analysed at the FAAM facility after the flight without any storage. However, given the time limitations, some other samples were analysed in the University of Leeds after being stored at about −18 °C for a few days, in a similar way to previous studies.[24,25,45,55,67] The set up in both cases was the same, and we did not observe any storing effect difference between samples collected on the same day that were analysed and the ones that were stored for a few days. INP measurement blank experiments were performed every day of analysis using a clean filter instead of an exposed filter. The water droplets placed on top of the filters with the aerosol samples nucleated ice at a significantly higher temperature than the blanks, as shown in Fig. S2.†

Note that this INP measurement technique was chosen instead of a filter washing droplet based assay[45] because the later one has a much smaller sensitivity to the sampled INPs (it places a much smaller fraction of aerosol particles of the filter in the same volume of water). Sensitivity to INP is important given the low sampling times that are possible during aircraft measurements. The disadvantage of the used droplet-on-filter assay is that we were not able to perform heating tests to detect the heat-labile component of the INP population, which is likely of biological origin. In spite of not relying on the filter-washing droplet based assay as a primary way to measure INP during this campaign, a subset of 10 of the polycarbonate filters were analysed using this technique. In 7 out of the 10 cases, only half of the filter was analysed using this method, reserving the other half for the SEM-EDS analysis. The separation was done using a clean sterile blade. A discussion of a comparison between these two techniques is shown in Sect. S3.† Overall, there is a good agreement for 6 samples, while other three present some discrepancies below an order of magnitude at some specific parts of the temperature spectrum. Only one sample presents a discrepancy of an order of magnitude. We suggest that the two techniques should be compared more formally in a future study using a more consistent set up such as an aerosol chamber. This could help to elucidate the discrepancies obtained in some occasions. However, the differences between the techniques do not modify the conclusions of this study.

2.4 Scanning electron microscopy

In order to quantify the size-resolved composition of the aerosol samples, individual aerosol particles collected on top of polycarbonate filters have been analysed using SEM-EDS, using an approach characterised by a previous study.[63] The Tescan Vega3 XM scanning electron microscope at the Leeds Electron Microscopy and Spectroscopy Centre was operated using an

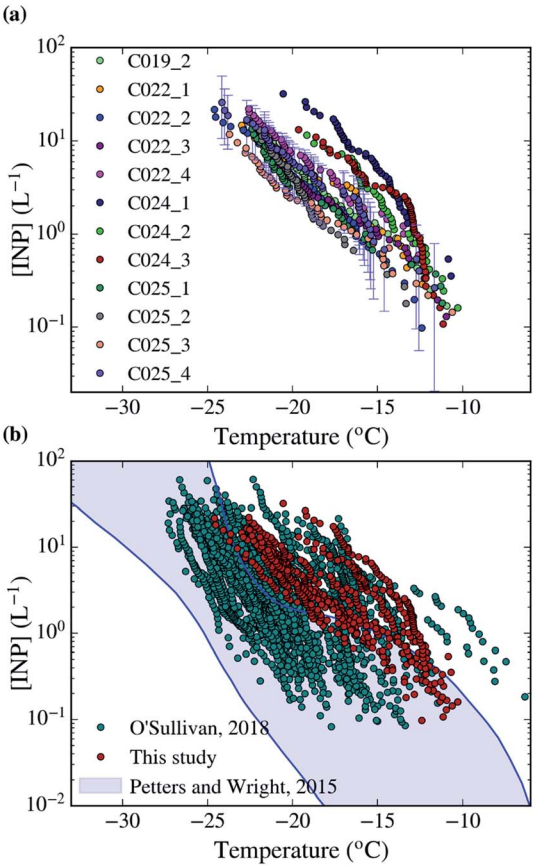

Fig. 2 [INP] of all the samples collected in this campaign analysed with the droplet-based assay described in Sect. 2.3.† The uncertainties of the calculations have been shown for one sample. (b) Comparison of the dataset collected in this study with a similar dataset collected in Northern England (O'Sullivan, 2018) and the range of observed [INP] in mid-latitude terrestrial environments.[45,68]

accelerating voltage of 20 keV, a pixel dwell time of 10 μs. The SEM has been operated using a software for automated particle analysis (AZtecFeature, Oxford Instruments). Filters were coated with 30 nm of Iridium prior to analysis to prevent the accumulation of electrons in the sample. Energy-Dispersive X-ray Spectroscopy was used to obtain the chemical composition of the aerosol particles. Each particle's raw X-ray spectra is matrix corrected and transformed by the software into weight percentage values of each element present in the analysis volume (typically 2 μm^3).

Polycarbonate filters (with a pore size of 0.4 μm) are placed under the microscope, and some areas of the filter are scanned using the software for automated particle analysis, which allows us to obtain the morphological properties as well as the chemical composition (using Energy-Dispersive X-ray Spectroscopy) of each aerosol particle of the scanned area in a semi-automated way. Morphological information is summarised in size-distributions, using the equivalent circular diameter of each particle, calculated from its cross-sectional area. In order to obtain the size-resolved compositional analysis, particles of each size bin are classified into 10 compositional categories, using the scheme described in a previous study.[63] All the results of the analysis are shown in Sect. 3.2.† Note that most particles classified in the Si only, Si rich, Al–Si rich and Ca rich have a chemical composition consistent with mineral dust.[63] The surface area of mineral dust in our samples was calculated by multiplying the surface area size distribution by the fraction of dust particles in each bin and then integrating the resulting curve.

3 Results and discussion

3.1 Ice-nucleating particle measurements

Using the droplet-on-filter assay described in Sect. 2.3,† we measured the INP concentration spectra of the collected aerosol samples, which are shown in Fig. 2a. The [INP] was calculated using eqn (1) and the fraction of droplets frozen from each filter experiment, which are shown in Fig. S2.† Most of the INP concentrations scatter over about half an order of magnitude for a given temperature. However, the measurements taken during the C024 flight have a steeper slope about −15 °C, and are about half an order of magnitude higher in [INP] than the rest for temperatures below −15 °C. All samples were collected around the South-East of the UK as shown in Fig. 1. Most of the samples were collected within the boundary layer. However, the origin of all the air masses on a multi-day time scale is the Atlantic Ocean, consistent with the prevailing winds in the region.

In order to better understand the types of INPs in this area, we quantified the correlation between the [INP] and different variables measured by the FAAM BAe-146 and our SEM-EDS analysis. This could show a potential link between the INP population and a specific aerosol type or atmospheric variable. However, we could not find any significant correlation in between [INP] and the observed variables. This is shown in Fig. S4,† where the [INP] of our samples at −19 °C has been plotted against the number of aerosol particles below and above ~3 μm (PCASP and CDP respectively), CO and O_3 concentration, altitude, area of the coarse and submicron modes measured by the PCASP and CDP, surface area of mineral dust measured using SEM-EDS and time overland (from the HYSPLIT analysis). A similar lack of correlation was found at other temperatures. Part of this low correlation is explained by the fact that the measured [INP] have relatively low variability, with most of the measured concentrations being consistent with each other considering the uncertainties. The only exception to this are the enhanced levels of O_3, submicron aerosol and mineral dust during the C024 flight, when INP concentrations were slightly higher. However, this is not enough to establish any causality. Given the shape of the INP spectra of the samples collected on that day, the enhancement could be produced by an increase in biological material, which might be linked to the overall enhancement in aerosol, particularly dust. Furthermore, the air masses associated with the C024 flight are different from the rest of the campaign, and they are more likely to be affected by continental Europe, as shown in Fig. 3. Additionally, Fig. S4† shows that most of the measurements were carried out within the boundary layer at altitudes from tens of

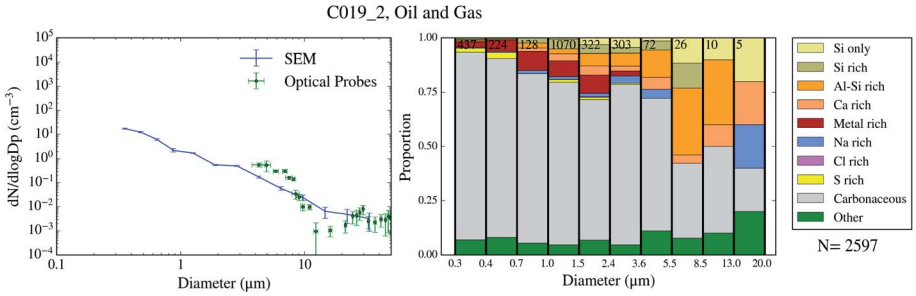

Fig. 3 Aerosol size distribution and size-resolved composition of the samples collected on 2017/07/11 (oil and gas). PCASP data not available for this flight due to technical problems.

meters to hundreds. There is no relation between altitude and [INP], suggesting that the INP population is relatively well mixed through the boundary layer, as expected.

The measured [INP] are compared in Fig. 2 with the ground-based INP measurements reported in Northern England during the autumn of 2016.[45] Our data is in the high-mid range of [INP] and has a slightly shallower slope than the data measured in Northern England. Additionally, the high [INP] reported at temperatures above ~−18 °C in Northern England were heat sensitive and therefore most likely proteinaceous biological INP.[45] It would appear that we sampled similar INP in this campaign, but we could not confirm this using heat tests (see Sect. 2.3† for the rationale of why we used this methodology). When compared with the range of observed [INP] in mid-latitude terrestrial environments, our measured concentrations yield above it or in the upper range.[68]

3.2 Aerosol with SEM

Using SEM-EDS, we collected the morphological properties of 35 677 particles as well as the chemical properties of a subset of 22 361 particles across 9 filters collected over 4 days of the campaign. The resulting size distributions and size-resolved compositions are shown in Fig. 3–6. We also compare the SEM size distributions with those derived from the optical probes on board of the FAAM BAe-146. The agreement between the optical and the SEM size distributions are generally good, although the SEM technique tends to undercount submicron aerosol, as previously observed in ref. 63. However, the coarser mode, which contributes dominantly to the surface area, is well captured in our filter samples.

The chemical composition of the collected aerosol particles doesn't exhibit a large sample-to-sample variability, as shown in Fig. 3–6. All the samples are dominated by carbonaceous

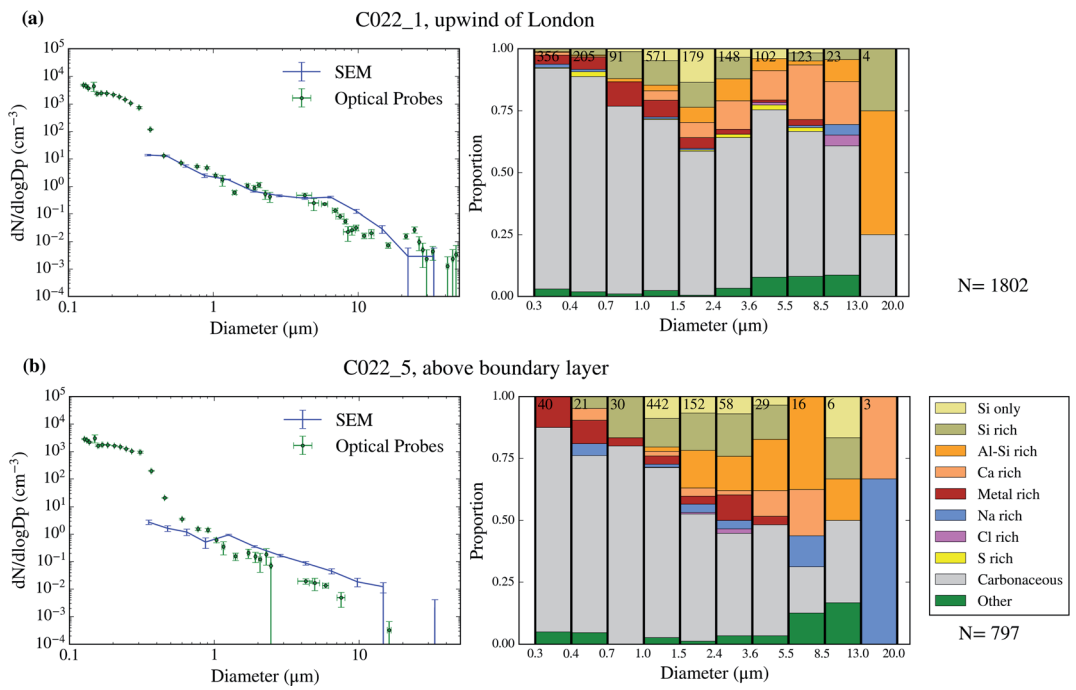

Fig. 4 Aerosol size distribution and size-resolved composition of the samples collected on 2017/07/17. The samples are C022_1 (a) and C022_5 (b).

particles in almost the whole size range. These particles have a chemical composition consistent with black carbon from combustion processes as well as primary or secondary organic material. All the samples have a prominent mineral dust mode (particles in the categories Si only, Si rich, Al–Si rich and Ca rich) centred in between ~1 and 10 μm, which constitute between 17 and 45% of the surface area of the samples, as shown in Table 1. In addition, there are minor contributions of sea spray aerosol (Na rich), metal rich particles and sulphates (S rich) in most samples. Biological aerosol particles were manually detected based on their morphology in nearly all samples. Further description of how the biological aerosol particles were detected is found in Sect. 3.4.† Almost all the samples were collected within the boundary layer. The lack of variability within the samples suggests that the aerosol particles were relatively well mixed within the boundary layer. The only exception is the C022_5, which was collected at about 1500 m, in the free troposphere. The chemical composition of this sample (Fig. 4b), was very similar to the rest of the samples. However, the particle number size distribution of this sample was smaller than most of the other SEM analysed samples, as shown in Fig. S5.† Unfortunately, [INP] was not measured for this sample due to technical problems during filter collection.

In order to investigate the composition of mineral dust sampled in the UK, we plot the ternary diagram of the chemical composition of the dust particles collected in this study. We also contrast this to results using the same technique for previously reported samples of Saharan dust from Barbados.[56] Note that for this analysis, dust refers to the particles in the categories Si only, Si rich, Al–Si rich, Ca rich and metal rich. Additionally, only Si, Al, Fe, Ca Mg and Na have been considered, excluding other elements. The majority of the particles in both datasets fall within a mode in the lower mid-section of the plot (about 50% of Si, 10% of Ca + Fe + Mg and 40% of Na + Al). Furthermore, both datasets exhibit some quartz particles (right corner of the ternary plots, corresponding to Si = 100%). The similarities between the datasets could be due to the fact that Saharan dust its commonly transported to North-Western Europe.[69] However, there are some differences between the two datasets. Fig. 7 clearly shows a significant presence of particles containing only Ca + Fe + Mg (top corner) in the UK samples that are not present in the samples collected in Barbados.

Further examination of these particles show that most of them contained only Ca (likely calcium carbonate), or Ca + S (likely Gypsum or sulphur aged calcium carbonate) which could have a local origin such a soil or construction.[70] Another difference between the datasets is that the UK dust particles are less concentrated in the central bottom mode, scattering more to other areas of the ternary plot such as the right side (corresponding to no Al or Na). Comparing the differences and similarities between the two datasets, it is likely the collected dust is a combination of dust from local and desert sources. The local sources of dust could include dust emitted from agricultural soils. These dusts have an ice-nucleation ability which is generally greater than desert dusts due to the presence of biological ice-nucleating material.[34–36]

3.3 The contribution of mineral dust to the INP population

As shown in Sect. 3.3† and Table 1, all the aerosol samples collected in the UK during this study contained significant amounts of dust particles (between 2.9 and 31.0 μm^2 cm^{-3}). In

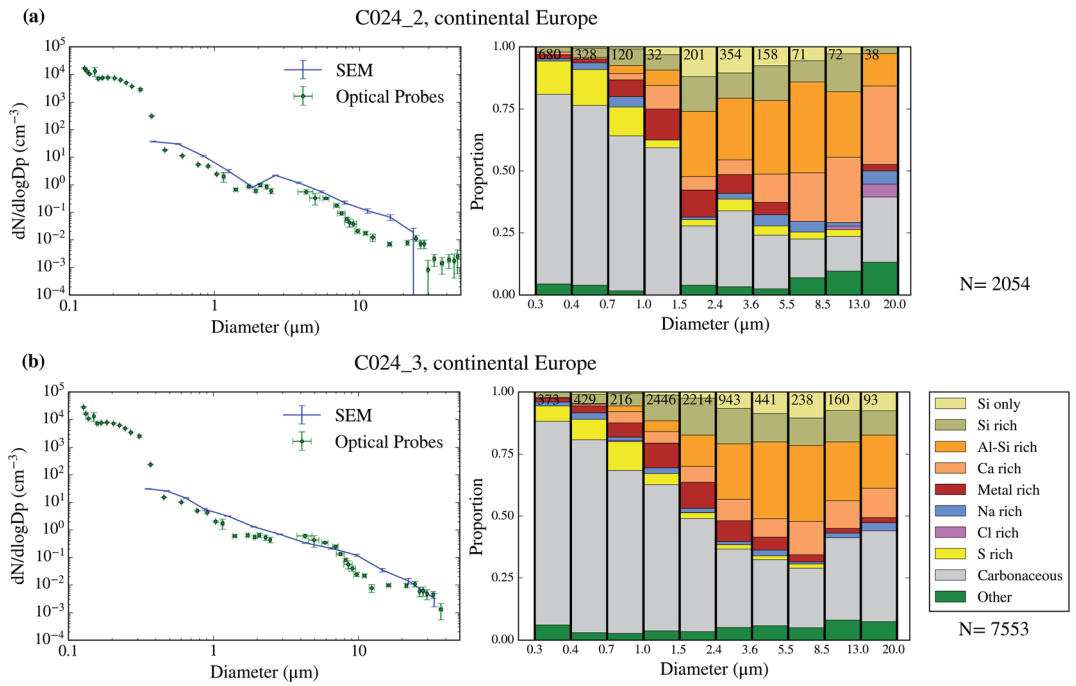

Fig. 5 Aerosol size distribution and size-resolved composition of the samples collected on 2017/07/19. The samples are C024_2 (a) and C024_3 (b).

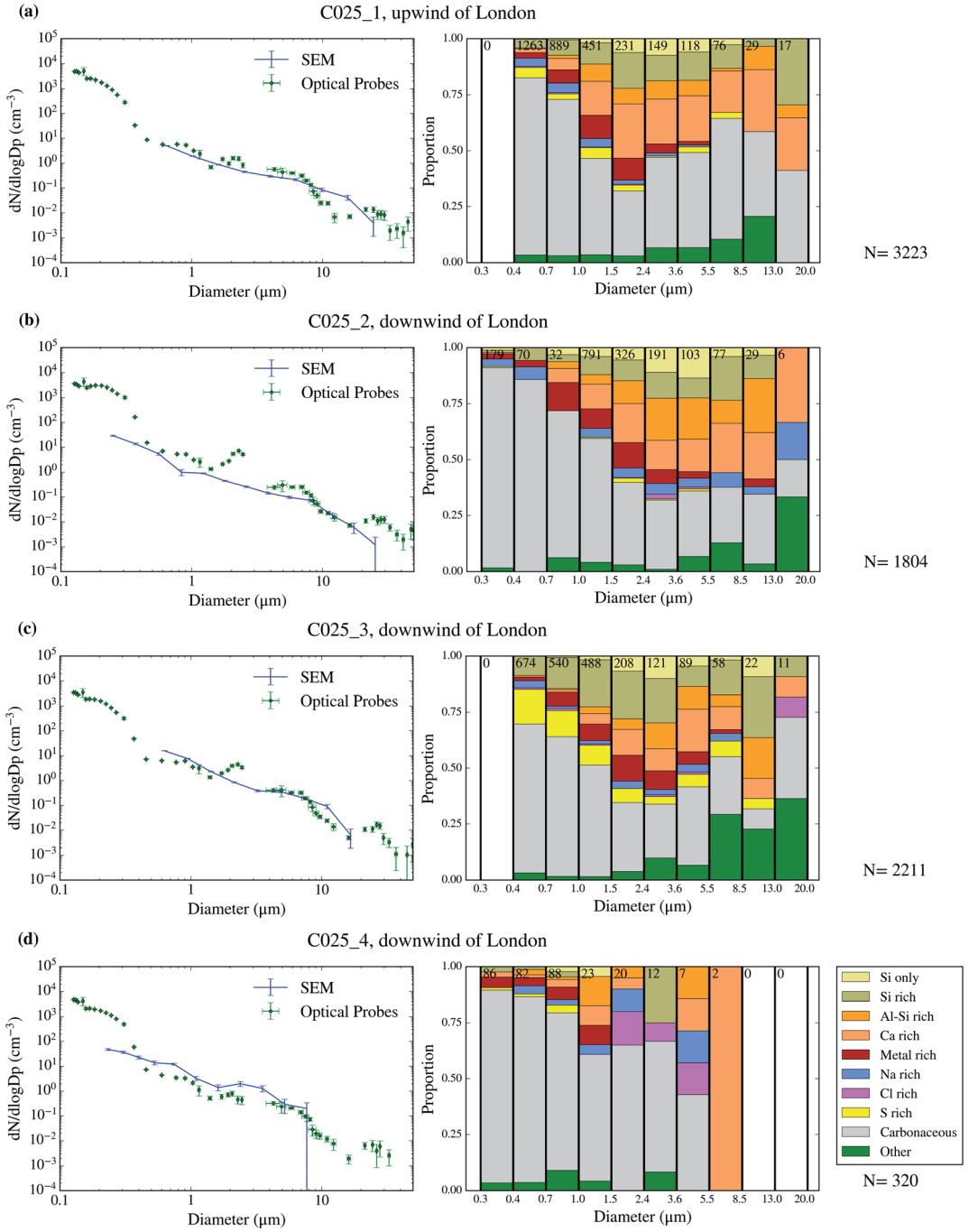

Fig. 6 Aerosol size distribution and size-resolved composition of the samples collected on 2017/07/20. The samples are C025_1 (a), C025_5 (b), C025_3 (c) and C025_4 (d). Due to technical problems, less aerosol particles were analysed for the C025_4 sample.

order to investigate if dust is contributing to the ice-nucleation ability of our samples, we calculate the ice-nucleation density of active sites (n_s) of the mineral dust component of the samples. This calculation assumes that all the ice-nucleation ability of our samples is given by the dust. If this assumption is valid, the derived n_s values should be compatible with mineral dust, whereas if the n_s for our sample is higher, then some other component must control the sample's ice-nucleating ability. We calculate n_s according to the equation:

$$n_s(T) = \frac{[\mathrm{INP}](T)}{s}$$

where s is the surface areas of the dust from Table 1, calculated using SEM-EDS. The n_s values of our samples are shown alongside n_s values of other Saharan dust (Fig. 8a) and agricultural soil (Fig. 8b) samples. The n_s values of our samples are larger (at the higher temperature range of their spectrum) and have a shallower slope than most of the Saharan dust samples (some of them scooped from the surface,[12,15,71] some sampled

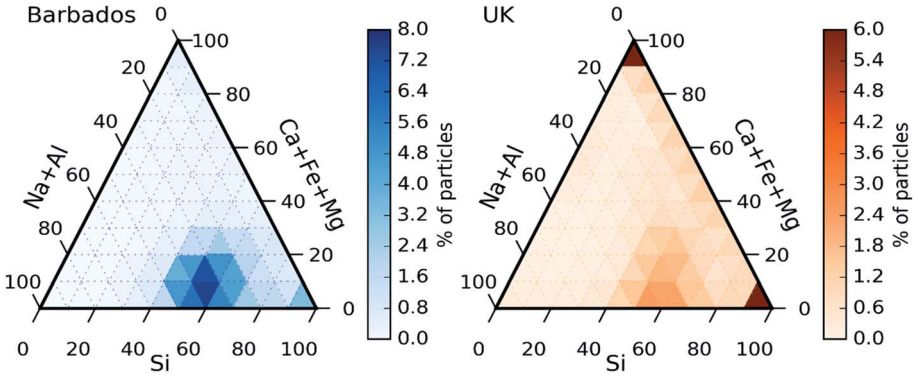

Fig. 7 Chemical composition in a heat map ternary diagram of Saharan dust particles collected in Barbados (a) compared with the dust particles collected in the UK in this study (b). The colour scale represents the percentage of particles of each dataset that are in each region of the ternary diagram.

from the air,[72,73] including one using a similar method to the present study[55]), as shown in Fig. 8a. This difference is almost 2 orders of magnitude at ~−15 °C. However, at temperatures below −20 °C, the n_s values of our samples overlap with the upper range of the desert dust data. Similarly, our samples exhibit larger n_s values than dust which contains 10% of K-feldspar, but they are compatible at temperatures at the end of the temperature range of our data (~−25 °C). Our samples exhibit a slightly larger activity than agricultural dusts at temperatures above ~−20 °C and a comparable below this threshold when compared with some of the data shown in Fig. 8b.[34,35] However, it has a similar slope and it is slightly less active than agricultural soils from another study.[36]

Overall, Fig. 8 shows that the upper range of the n_s of desert dust could explain the ice-nucleation ability at the colder end of its temperature range (−20 to −25 °C). However, an additional type of aerosol particle is responsible for ice-nucleation at temperatures close to −20 °C and above. Given that agricultural dust is likely one of the components of the dust in the samples, a part of this enhancement could be due to the presence of organic material within the soil. However, it is also likely that an additional types of INPs within our samples is responsible for its high ice-nucleation ability at the higher temperature range. This additional contribution to the INP population could be primary biological aerosol particles. Biological aerosol particles were detected in nearly all samples by SEM (see Sect. 3.4†). It is also worth noting that the results shown here are consistent with the findings of other INP measurements in the UK. In a previous study, the [INP] of samples collected in autumn in North England were consistent with the modelled dust [INP] at temperatures below −20 °C, while concentrations above that temperature were heat-sensitive (likely biogenic) and larger than expected from the modelled desert dust.[45] Hence, by inference, we suggest that the enhanced activity of the samples above −20 °C could be related to heat-sensitive protein-based biogenic (primary biological particles, by-product fragments and macromolecules) ice-nucleating material.

3.4 Estimates of primary biological aerosol particles

Biological aerosol particles are commonly found in the atmosphere, particularly in places such as agricultural managed areas like the UK.[74–77] Some of these particles are known to nucleate ice and therefore they have the potential to contribute to the INP population.[1] Primary biological aerosol particles, in

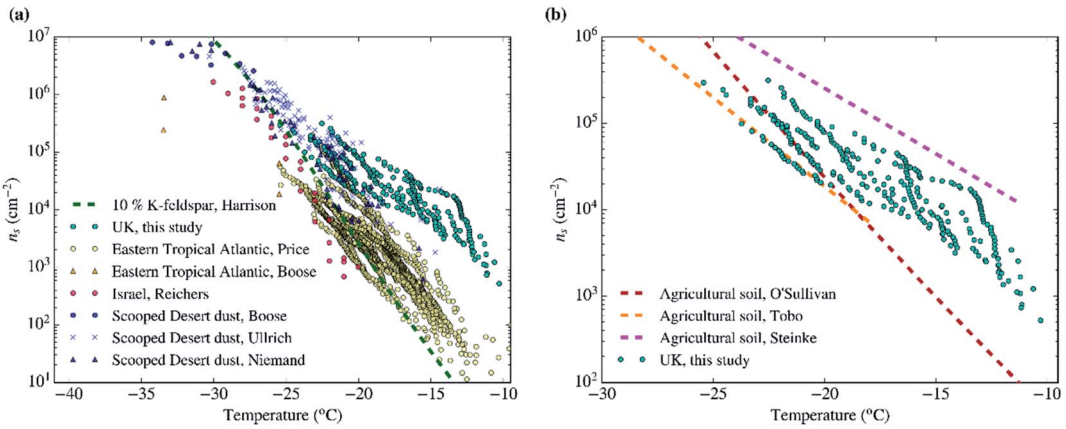

Fig. 8 Ice active site densities (n_s) of the samples collected in the UK assuming that only their mineral dust component is responsible for ice-nucleation. (a) The data is compared to Saharan dust from different studies,[12,15,55,71–73] as well as dust containing 10% of K-feldspar.[87] (b) Our n_s values are shown in comparison with agricultural soils from different studies.[34–36]

the form of supermicron cells or plant fragments, were detected in all the SEM-EDS analysed samples.

Primary biological particles were detected by manually scanning the SEM images looking for the distinct morphologies of biological aerosol particles on the filters. A selection of some of the different biological aerosol particles is shown in Fig. 9 and a set of the images of ~100 particles is shown in Sect. S6.† The majority of the identified particles are ellipsoidal (a–d, f–h, k), and can present a smooth (h and k) or ornamented surface (a–d) although some of them have a spheroid (e), or shell shape (i and j). Some of them can present certain asymmetry with respect to their major axis (f–k). Most of them seemed to be deposited on the filter individually while some others appear in pairs or clusters of several particles (normally attached at their extremes). On some occasions, narrow and long particles (tens of μm) were observed (l). Based on their morphology, the majority of the particles detected here are consistent with fungal spores such as conidia, ascospores or hyphal fragments, as reported by other studies of SEM-EDS on biological aerosols.[78–80]

Some of the presented particles are consistent with fungal spores of different genuses.[81] We found particles that are consistent with fungal spores of the *Cladosporium* species-complex (a–d). Spores that could belong to the *Aspergillus* or *Penicilinum* genera (e, f, i and j) were identified. (h) Likely belongs to the *Botrytis* genus. Some particles are more difficult to classify down to the genus level but are consistent with basidiospores (g and j) or ascospores (k). The large filamentous particle in (l) is likely a fragment of fungal hyphae. Additionally, we cannot rule out the possibility of bacterial aerosol in our samples, such as (i). Overall, most of the spores we found belong to the *Cladosporium*, *Aspergillus* and *Penicillinium*

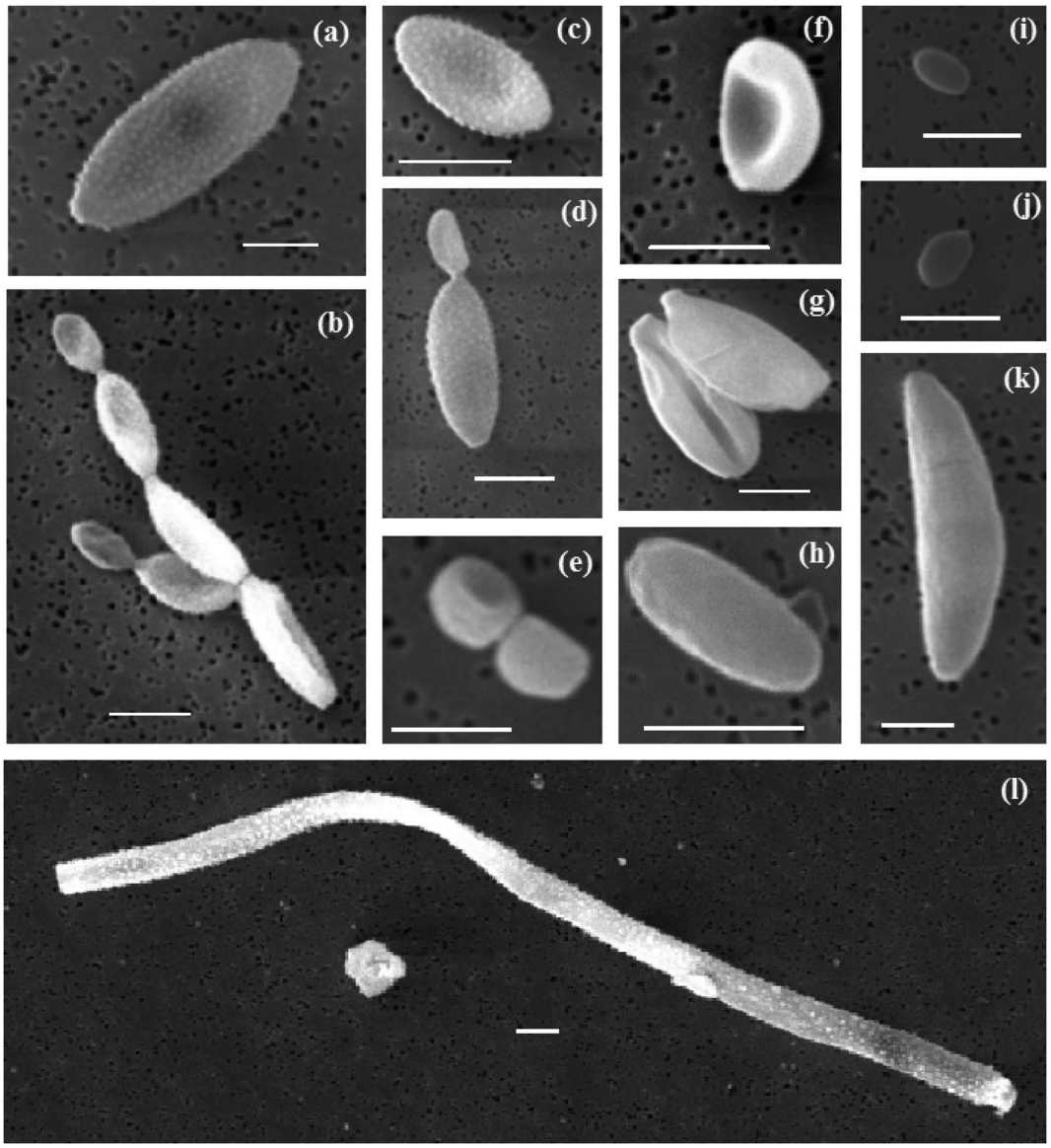

Fig. 9 Different biological aerosol particles observed on top of the filters presented in this study. A selection of the most representative biological aerosol particles has been presented. The scale corresponds to 5 μm in all the images.

genera, which are very commonly found near the ground, sometimes in the soil, on plants and plant debris. Spores of the genera *Botrytis*, *Didymella* and *Mycosphaerella graminicola*, which are produced on plants, and plant debris or soil, were also found (see Sect. S6†). The presence of these spores demonstrates that there is a substantial source of terrestrial aerosol particles. In Fig. 1b it is shown that apart from flight CO22, back-trajectories of air masses were predominantly over the sea before reaching the British Isles and so it can be deduced that the genera sampled most likely came from ground sources in Britain and Ireland. Flight CO22 back-trajectories included locations over northern France, Belgium and the Netherlands and so could have received spores from sources in those locations.

EDS analysis was applied to some of the detected biological aerosol particles. Our SEM-EDS approach cannot be used to quantify the percentage of C and O in the particle, since these elements are present in the background polycarbonate filter.[63] As a consequence, we cannot fully quantify the exact chemical composition of these biological aerosol particles. Additionally, since the characteristic X-rays of P and the coating of the samples (Ir) overlap, our technique is likely to miss the detection of P in the particles. Background elements (C and O) were the dominant components in most of the detected biological aerosol particles. However, the majority of the particles also exhibited the presence of elements such as K, S, Ca, Cl, P or Na (in that order of frequency). Elements such as Si, Al or Fe were detected in some rare occasions. The observed chemical composition is consistent with previous studies.[82,83]

Up to tens of particles with these morphological characteristics were detected in all the SEM-EDS analysis we carried out on the filters (each of the analysis covers up to 1% of the filter surface). This allowed us to quantify a lower limit of the biological aerosol concentration per surface of the filter as well as their atmospheric concentration. In order to determine if these particles are potential artefacts, we performed a handling blank experiment during a test flight in the UK in September 2017, which is shown in Fig. 10a. In this experiment, a pair of filters (measurement 1 and 2) were exposed to the air for a few minutes, sampling myriads of aerosol particles. Additionally, one handling blank was placed in the system and treated as a normal filter but not exposed to the air. There was a significantly larger amount of biological aerosol particles in the filters exposed to the atmosphere (measurement 1 and 2) than in the handling blank filter (where there was less than 1 biological particle per mm^2). Fig. 10a also shows that there was a significant amount of biological particles within most of the filters collected for this study (in between 5 and 30 particles per mm^2). In Fig. 10b, these biological particles are reported in terms of atmospheric concentration. Almost all of our measurements of the concentration of primary biological aerosol particles bigger than ~2 μm, with obvious biological morphological features, are between about 5 and 100 L^{-1}. These values are consistent with the literature data for fungal spores over vegetated regions.[75] The only measurement within the dataset presented here where the biological aerosol particle concentration is not significantly larger than the handling blank is C022_5. This sample was collected at a higher altitude than the rest, about 1500 m and above the boundary layer. Our results indicate that there was a significant amount of primary biological aerosol particles (10–100 L^{-1}) within the Northern-West European boundary layer during July of 2017. However, more research is necessary in order to study if these particles are also present in the free troposphere.

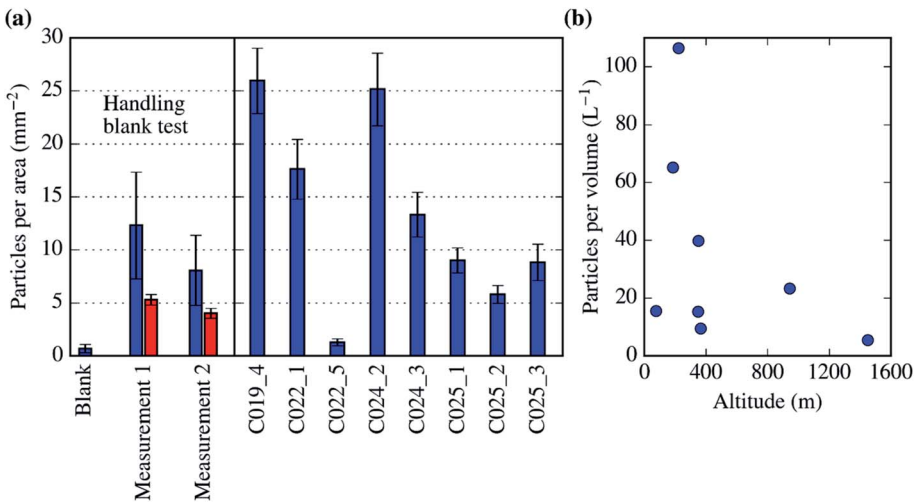

Fig. 10 Estimation of the concentrations of biological aerosol particles. (a) Biological particle concentration per unit of area in the filter. The first 3 bars correspond to the handling blank test carried out on the 27th of September of 2017. In this test, a handling blank as well as two samples were collected (measurement 1 and 2). The number of biological aerosol particles on top of the measurements was much higher than in the handling blank. The data in the red bar corresponds to a second analysis using a very low magnification, which underestimates the detection of biological aerosol particles. (b) Atmospheric concentrations of biological aerosol particles of the SEM-EDS analysed filters (from C019_4 to C025_3). The data has been presented alongside pressure altitude. Note that the data point in the bottom right side of the image (about 1500 m) corresponds to the low biological aerosol sample (C022_5).

Our approach to quantifying the concentration of primary biological aerosol particles will likely underestimate the real concentrations given that some of these particles would not be counted if they did not show any of the obvious biological morphological features. This visual technique was only sensitive to particles bigger than ~2 μm. Hence, we are not sensitive to most bacteria, which tend to be smaller and have a smooth spherical or oval morphology, which makes it challenging to identify them on the basis of images alone. In addition, we cannot establish whether the biological particles that we have belong to species that nucleate ice effectively. Our techniques cannot be used to determine if the detected biological aerosol particles significantly contribute to the INP population. However, if a fraction of ~0.001 to 0.01 of the biological particles present in our samples are active as INPs at the high end of the temperature range of the measurements (−10 to −15 °C), they could be responsible for the measured [INP] (~0.1 to 1 L^{-1}). Some studies suggest that for fungal several types of common fungal spores, those fractions of INPs are only reached at lower temperatures (below −20 °C).[28,40,84] However, the ice-nucleation properties of fungal material are very complex and variable, showing remarkably high freezing temperatures in some occasions.[85] Additionally, other types of primary biological aerosol particles could also exist in our samples. In conclusion, it is unclear whether the detected primary biological aerosol particles contribute to the measured INP population. However, the observation of these particles does demonstrate that there is a local source (or sources) of terrestrial biological aerosol, which may explain the enhanced ice nucleating activity of these samples.

4 Conclusions

In July of 2017, aerosol particles were sampled on top of filters during a set of flights carried out by the FAAM BAe-146 over the South-East of the UK. Particles up to ~20 μm were collected using the filter inlet system on board of the aircraft,[63] which allowed us to collected aerosol samples onto two different filters in parallel. These filters were analysed using SEM-EDS and a droplet-based assay in order to quantify the size-resolved composition and [INP] of the aerosol sample.

The measured [INP] did not exhibit a large variability during the course of the campaign. Additionally, the reported values are in the upper end of other measurements in similar latitudes. The SEM-EDS analysis suggests that all the samples had similar morphological and chemical characteristics. Furthermore, they were dominated by carbonaceous aerosol particles, with a strong presence of mineral dust particles, particularly in the coarse sizes. The surface areas of the detected dust were between 2.9 and 31.0 $\mu m^2\ cm^{-3}$ (between 17 and 45% of the surface area of the samples). Although we cannot fully determine the origin of these dust particles, a significant part of them could be transported desert dust with contributions of material from other sources, potentially local fertile soils which are known to contain very active components.[34] Primary biological particles, bigger than 2 μm and of and possessing an obvious biological morphology, were detected in all the samples with concentrations of 5 to 100 L^{-1}.

Further analysis shows that the ice-nucleation ability of our samples is consistent with mineral dust at the lower end of its temperature spectrum (close to −25 °C). However, at temperatures above −20 °C, our samples are significantly more active than expected from desert dust, being enhanced by almost 2 orders of magnitude at ~−15 °C. A part of the measured dust is likely to have another origin than deserts, and it could include fertile soils, which contain biological residues and can have a higher ice-nucleation ability than desert dust. Additionally, since primary biological aerosol particles were detected in most samples, there is an active source (or sources) of aerosol from the terrestrial environment. Hence, it is likely that the enhancement in the ice-nucleation ability at the higher end of the temperature spectrum is produced by the presence of biological material.

Our measurements have been carried out in July and mostly within the boundary layer. At these locations, altitudes and time of the year, temperatures rarely reach 0 °C, hence shallow mixed-phase clouds are very infrequent. However, they have been conducted at different altitudes covering most of the boundary layer. As a consequence, our results are representative of the boundary layer and are unlikely to be affected by being too close to ground level sources of INPs. This is particularly relevant for the biological aerosol particle measurements, which are usually carried out close to where these aerosol particles are emitted. Additionally, boundary layer INPs might play a role in the evolution of convective clouds, which frequently occur in this region at this time of the year.[4,86] Our results suggest that biological INPs may be an important INP type in higher temperature freezing in these convective systems. In addition, our measurements are consistent with the existing body of atmospheric measurements which emphasise the importance of mineral dust and biological material as INPs at the lower and higher end of the temperature spectrum, respectively.

Author contributions

The fieldwork was planned by ASM with the help of JBM and BJM. ASM carried out the aerosol collection with the help of JBM. All the experiments (INP analysis and SEM-EDS) were carried out by ASM. The analysis of the data was carried out by ASM, with the help of ITB and BJM. The analysis and detection of biological aerosol particles were carried out by ASM and JSW. ASM wrote the manuscript with contributions of all the co-authors.

Conflicts of interest

There are no conflicts to declare.

Acknowledgements

We are thankful to Mark D. Tarn for delivering laboratory consumables to us during the execution of the campaign.

Airborne data and filter samples were acquired using the FAAM BAe-146-301 Atmospheric Research Aircraft, flown by Airtask Ltd and managed by FAAM Airborne Laboratory, jointly operated by UKRI and the University of Leeds. We thank all the people involved in the EMERGE campaign and the Oil and Gas flights we took part in, as well as Avalon. We acknowledge the Centre for Environmental Data Analysis for providing us with the FAAM datasets used here and the Leeds Electron Microscopy and Spectroscopy Centre for the use of their microscopy facilities. We are grateful to the European Research Council (648661 MarineIce) and the Natural Environment Research Council (NE/T00648X/1 M-phase) for funding.

References

1 B. J. Murray, D. O'Sullivan, J. D. Atkinson and M. E. Webb, Ice nucleation by particles immersed in supercooled cloud droplets, *Chem. Soc. Rev.*, 2012, **41**(19), 6519–6554.

2 C. Hoose and O. Mohler, Heterogeneous ice nucleation on atmospheric aerosols: a review of results from laboratory experiments, *Atmos. Chem. Phys.*, 2012, **12**(20), 9817–9854.

3 J. Vergara-Temprado, A. K. Miltenberger, K. Furtado, D. P. Grosvenor, B. J. Shipway, A. A. Hill, *et al.*, Strong control of Southern Ocean cloud reflectivity by ice-nucleating particles, *Proc. Natl. Acad. Sci. U. S. A.*, 2018, **115**(11), 2687–2692.

4 J. W. Taylor, T. W. Choularton, A. M. Blyth, Z. Liu, K. N. Bower, J. Crosier, *et al.*, Observations of cloud microphysics and ice formation during COPE, *Atmos. Chem. Phys.*, 2016, **16**(2), 799–826.

5 R. E. Hawker, A. K. Miltenberger, J. M. Wilkinson, A. A. Hill, B. J. Shipway, Z. Cui, *et al.*, The nature of ice-nucleating particles affects the radiative properties of tropical convective cloud systems, *Atmos. Chem. Phys. Discuss.*, 2020, **2020**, 1–39.

6 M. Komurcu, T. Storelvmo, I. Tan, U. Lohmann, Y. Yun, J. E. Penner, *et al.*, Intercomparison of the cloud water phase among global climate models, *J. Geophys. Res.: Atmos.*, 2014, **119**(6), 3372–3400.

7 D. T. McCoy, I. Tan, D. L. Hartmann, M. D. Zelinka and T. Storelvmo, On the relationships among cloud cover, mixed-phase partitioning, and planetary albedo in GCMs, *J. Adv. Model. Earth Syst.*, 2016, **8**(2), 650–668.

8 D. T. McCoy, D. L. Hartmann and M. D. Zelinka, Chapter 9 - Mixed-Phase Cloud Feedbacks, in *Mixed-Phase Clouds*, ed. C. Andronache, Elsevier, 2018, pp. 215–236.

9 T. Storelvmo, I. Tan and A. V. Korolev, Cloud Phase Changes Induced by CO_2 Warming—a Powerful yet Poorly Constrained Cloud-Climate Feedback, *Curr. Clim. Change Rep.*, 2015, **1**(4), 288–296.

10 B. J. Murray, K. S. Carslaw and P. R. Field, Opinion: Cloud-phase climate feedback and the importance of ice-nucleating particles, *Atmos. Chem. Phys.*, 2021, **21**(2), 665–679.

11 P. Ceppi, F. Brient, M. D. Zelinka and D. L. Hartmann, Cloud feedback mechanisms and their representation in global climate models, *Wiley Interdiscip. Rev. Clim. Change*, 2017, **8**(4), e465.

12 M. Niemand, O. Mohler, B. Vogel, H. Vogel, C. Hoose, P. Connolly, *et al.*, A Particle-Surface-Area-Based Parameterization of Immersion Freezing on Desert Dust Particles, *J. Atmos. Sci.*, 2012, **69**(10), 3077–3092.

13 J. D. Atkinson, B. J. Murray, M. T. Woodhouse, T. F. Whale, K. J. Baustian, K. S. Carslaw, *et al.*, The importance of feldspar for ice nucleation by mineral dust in mixed-phase clouds, *Nature*, 2013, **498**(7454), 355–358.

14 J. Vergara-Temprado, B. J. Murray, T. W. Wilson, D. O'Sullivan, J. Browse, K. J. Pringle, *et al.*, Contribution of feldspar and marine organic aerosols to global ice nucleating particle concentrations, *Atmos. Chem. Phys.*, 2017, **17**(5), 3637–3658.

15 R. Ullrich, C. Hoose, O. Mohler, M. Niemand, R. Wagner, K. Hohler, *et al.*, A New Ice Nucleation Active Site Parameterization for Desert Dust and Soot, *J. Atmos. Sci.*, 2017, **74**(3), 699–717.

16 N. Huneeus, M. Schulz, Y. Balkanski, J. Griesfeller, J. Prospero, S. Kinne, *et al.*, Global dust model intercomparison in AeroCom phase I, *Atmos. Chem. Phys.*, 2011, **11**(15), 7781–7816.

17 P. Ginoux, J. M. Prospero, T. E. Gill, N. C. Hsu and M. Zhao, Global-scale attribution of anthropogenic and natural dust sources and their emission rates based on MODIS Deep Blue aerosol products, *Rev. Geophys.*, 2012, **50**(3), 1–36.

18 J. E. Bullard, M. Baddock, T. Bradwell, J. Crusius, E. Darlington, D. Gaiero, *et al.*, High-latitude dust in the Earth system, *Rev. Geophys.*, 2016, **54**(2), 447–485.

19 T. P. Mangan, J. D. Atkinson, J. W. Neuberg, D. O'Sullivan, T. W. Wilson, T. F. Whale, *et al.*, Heterogeneous Ice Nucleation by Soufriere Hills Volcanic Ash Immersed in Water Droplets, *PLoS One*, 2017, **12**(1), e0169720.

20 L. G. Jahn, W. D. Fahy, D. B. Williams and R. C. Sullivan, Role of Feldspar and Pyroxene Minerals in the Ice Nucleating Ability of Three Volcanic Ashes, *ACS Earth Space Chem.*, 2019, **3**(4), 626–636.

21 E. C. Maters, D. B. Dingwell, C. Cimarelli, D. Muller, T. F. Whale and B. J. Murray, The importance of crystalline phases in ice nucleation by volcanic ash, *Atmos. Chem. Phys.*, 2019, **19**(8), 5451–5465.

22 E. C. Maters, C. Cimarelli, A. S. Casas, D. B. Dingwell and B. J. Murray, Volcanic ash ice-nucleating activity can be enhanced or depressed by ash-gas interaction in the eruption plume, *Earth Planet. Sci. Lett.*, 2020, **551**, 116587.

23 T. W. Wilson, L. A. Ladino, P. A. Alpert, M. N. Breckels, I. M. Brooks, J. Browse, *et al.*, A marine biogenic source of atmospheric ice-nucleating particles, *Nature*, 2015, **525**(7568), 234–238.

24 P. J. DeMott, T. C. Hill, C. S. McCluskey, K. A. Prather, D. B. Collins, R. C. Sullivan, *et al.*, Sea spray aerosol as a unique source of ice nucleating particles, *Proc. Natl. Acad. Sci. U. S. A.*, 2016, **113**(21), 5797–5803.

25 C. S. McCluskey, J. Ovadnevaite, M. Rinaldi, J. D. Atkinson, F. Belosi, D. Ceburnis, *et al.*, Marine and Terrestrial Organic Ice-Nucleating Particles in Pristine Marine to

Continentally Influenced Northeast Atlantic Air Masses, *J. Geophys. Res.: Atmos.*, 2018, **123**(11), 6196–6212.

26 L. Ickes, G. C. E. Porter, R. Wagner, M. P. Adams, S. Bierbauer, A. K. Bertram, *et al.*, Arctic marine ice nucleating aerosol: a laboratory study of microlayer samples and algal cultures, *Atmos. Chem. Phys.*, 2020, **20**(18), 11089–11117.

27 B. G. Pummer, H. Bauer, J. Bernardi, S. Bleicher and H. Grothe, Suspendable macromolecules are responsible for ice nucleation activity of birch and conifer pollen, *Atmos. Chem. Phys.*, 2012, **12**(5), 2541–2550.

28 D. I. Haga, S. M. Burrows, R. Iannone, M. J. Wheeler, R. H. Mason, J. Chen, *et al.*, Ice nucleation by fungal spores from the classes Agaricomycetes, Ustilaginomycetes, and Eurotiomycetes, and the effect on the atmospheric transport of these spores, *Atmos. Chem. Phys.*, 2014, **14**(16), 8611–8630.

29 H. Wex, S. Augustin-Bauditz, Y. Boose, C. Budke, J. Curtius, K. Diehl, *et al.*, Intercomparing different devices for the investigation of ice nucleating particles using Snomax® as test substance, *Atmos. Chem. Phys.*, 2015, **15**(3), 1463–1485.

30 B. G. Pummer, C. Budke, S. Augustin-Bauditz, D. Niedermeier, L. Felgitsch, C. J. Kampf, *et al.*, Ice nucleation by water-soluble macromolecules, *Atmos. Chem. Phys.*, 2015, **15**(8), 4077–4091.

31 D. O'Sullivan, B. J. Murray, J. F. Ross, T. F. Whale, H. C. Price, J. D. Atkinson, *et al.*, The relevance of nanoscale biological fragments for ice nucleation in clouds, *Sci. Rep.*, 2015, **5**, 8082.

32 S. Augustin-Bauditz, H. Wex, C. Denjean, S. Hartmann, J. Schneider, S. Schmidt, *et al.*, Laboratory-generated mixtures of mineral dust particles with biological substances: characterization of the particle mixing state and immersion freezing behavior, *Atmos. Chem. Phys.*, 2016, **16**(9), 5531–5543.

33 D. O'Sullivan, B. J. Murray, J. F. Ross and M. E. Webb, The adsorption of fungal ice-nucleating proteins on mineral dusts: a terrestrial reservoir of atmospheric ice-nucleating particles, *Atmos. Chem. Phys.*, 2016, **16**(12), 7879–7887.

34 D. O'Sullivan, B. J. Murray, T. L. Malkin, T. F. Whale, N. S. Umo, J. D. Atkinson, *et al.*, Ice nucleation by fertile soil dusts: relative importance of mineral and biogenic components, *Atmos. Chem. Phys.*, 2014, **14**(4), 1853–1867.

35 Y. Tobo, P. J. DeMott, T. C. J. Hill, A. J. Prenni, N. G. Swoboda-Colberg, G. D. Franc, *et al.*, Organic matter matters for ice nuclei of agricultural soil origin, *Atmos. Chem. Phys.*, 2014, **14**(16), 8521–8531.

36 I. Steinke, R. Funk, J. Busse, A. Iturri, S. Kirchen, M. Leue, *et al.*, Ice nucleation activity of agricultural soil dust aerosols from Mongolia, Argentina, and Germany, *J. Geophys. Res.: Atmos.*, 2016, **121**(22), 13559–13576.

37 W. T. K. Huang, L. Ickes, I. Tegen, M. Rinaldi, D. Ceburnis and U. Lohmann, Global relevance of marine organic aerosol as ice nucleating particles, *Atmos. Chem. Phys.*, 2018, **18**(15), 11423–11445.

38 C. S. McCluskey, P. J. DeMott, P. L. Ma and S. M. Burrows, Numerical Representations of Marine Ice-Nucleating Particles in Remote Marine Environments Evaluated Against Observations, *Geophys. Res. Lett.*, 2019, **46**(13), 7838–7847.

39 C. Hoose, J. E. Kristjánsson and S. M. Burrows, How important is biological ice nucleation in clouds on a global scale?, *Environ. Res. Lett.*, 2010, **5**(2), 024009.

40 D. I. Haga, R. Iannone, M. J. Wheeler, R. Mason, E. A. Polishchuk, T. Fetch, *et al.*, Ice nucleation properties of rust and bunt fungal spores and their transport to high altitudes, where they can cause heterogeneous freezing, *J. Geophys. Res.: Atmos.*, 2013, **118**(13), 7260–7272.

41 A. Sesartic, U. Lohmann and T. Storelvmo, Modelling the impact of fungal spore ice nuclei on clouds and precipitation, *Environ. Res. Lett.*, 2013, **8**(1), 014029.

42 M. Sahyoun, H. Wex, U. Gosewinkel, T. Šantl-Temkiv, N. W. Nielsen, K. Finster, *et al.*, On the usage of classical nucleation theory in quantification of the impact of bacterial INP on weather and climate, *Atmos. Environ.*, 2016, **139**, 230–240.

43 M. Hummel, C. Hoose, B. Pummer, C. Schaupp, J. Fröhlich-Nowoisky and O. Möhler, Simulating the influence of primary biological aerosol particles on clouds by heterogeneous ice nucleation, *Atmos. Chem. Phys.*, 2018, **18**(20), 15437–15450.

44 Z. A. Kanji, L. A. Ladino, H. Wex, Y. Boose, M. Burkert-Kohn, D. J. Cziczo, *et al.*, Overview of Ice Nucleating Particles, *Meteorol. Monogr.*, 2017, **58**, 1–33.

45 D. O'Sullivan, M. P. Adams, M. D. Tarn, A. D. Harrison, J. Vergara-Temprado, G. C. E. Porter, *et al.*, Contributions of biogenic material to the atmospheric ice-nucleating particle population in North Western Europe, *Sci. Rep.*, 2018, **8**(1), 13821.

46 L. A. Ladino, G. B. Raga, H. Alvarez-Ospina, M. A. Andino-Enríquez, I. Rosas, L. Martínez, *et al.*, Ice-nucleating particles in a coastal tropical site, *Atmos. Chem. Phys.*, 2019, **19**(9), 6147–6165.

47 E. Garcia, T. C. J. Hill, A. J. Prenni, P. J. DeMott, G. D. Franc and S. M. Kreidenweis, Biogenic ice nuclei in boundary layer air over two U.S. High Plains agricultural regions, *J. Geophys. Res.: Atmos.*, 2012, **117**, D18209.

48 R. D. Borys, Studies of ice nucleation by Arctic aerosol on AGASP-II, *J. Atmos. Chem.*, 1989, **9**(1–3), 169–185.

49 D. C. Rogers, P. J. DeMott and S. M. Kreidenweis, Airborne measurements of tropospheric ice-nucleating aerosol particles in the Arctic spring, *J. Geophys. Res.: Atmos.*, 2001, **106**(D14), 15053–15063.

50 A. J. Prenni, P. J. Demott, D. C. Rogers, S. M. Kreidenweis, G. M. McFarquhar, G. Zhang, *et al.*, Ice nuclei characteristics from M-PACE and their relation to ice formation in clouds, *Tellus B*, 2009, **61**(2), 436–448.

51 M. Hartmann, K. Adachi, O. Eppers, C. Haas, A. Herber, R. Holzinger, *et al.*, Wintertime Airborne Measurements of Ice Nucleating Particles in the High Arctic: A Hint to a Marine, Biogenic Source for Ice Nucleating Particles, *Geophys. Res. Lett.*, 2020, **47**(13), e2020GL087770.

52 P. R. Field, A. J. Heymsfield, B. J. Shipway, P. J. DeMott, K. A. Pratt, D. C. Rogers, *et al.*, Ice in Clouds Experiment–

Layer Clouds. Part II: Testing Characteristics of Heterogeneous Ice Formation in Lee Wave Clouds, *J. Atmos. Sci.*, 2012, **69**(3), 1066–1079.

53 R. C. Schnell, Airborne ice nucleus measurements around the Hawaiian Islands, *J. Geophys. Res.*, 1982, **87**(C11), 8886.

54 J. L. Stith, V. Ramanathan, W. A. Cooper, G. C. Roberts, P. J. DeMott, G. Carmichael, *et al.*, An overview of aircraft observations from the Pacific Dust Experiment campaign, *J. Geophys. Res.*, 2009, **114**, D05207.

55 H. C. Price, K. J. Baustian, J. B. McQuaid, A. Blyth, K. N. Bower, T. Choularton, *et al.*, Atmospheric Ice-Nucleating Particles in the Dusty Tropical Atlantic, *J. Geophys. Res.: Atmos.*, 2018, **123**(4), 2175–2193.

56 A. Sanchez-Marroquin, O. Arnalds, K. J. Baustian-Dorsi, J. Browse, P. Dagsson-Waldhauserova, A. D. Harrison, *et al.*, Iceland is an episodic source of atmospheric ice-nucleating particles relevant for mixed-phase clouds, *Sci. Adv.*, 2020, **6**(26), eaba8137.

57 J. Schrod, D. Weber, J. Drücke, C. Keleshis, M. Pikridas, M. Ebert, *et al.*, Ice nucleating particles over the Eastern Mediterranean measured by unmanned aircraft systems, *Atmos. Chem. Phys.*, 2017, **17**(7), 4817–4835.

58 P. D. Rosenberg, A. R. Dean, P. I. Williams, J. R. Dorsey, A. Minikin, M. A. Pickering, *et al.*, Particle sizing calibration with refractive index correction for light scattering optical particle counters and impacts upon PCASP and CDP data collected during the Fennec campaign, *Atmos. Meas. Tech.*, 2012, **5**(5), 1147–1163.

59 C. Chou, P. Formenti, M. Maille, P. Ausset, G. Helas, M. Harrison, *et al.*, Size distribution, shape, and composition of mineral dust aerosols collected during the African Monsoon Multidisciplinary Analysis Special Observation Period 0: Dust and Biomass-Burning Experiment field campaign in Niger, January 2006, *J. Geophys. Res.: Atmos.*, 2008, **113**(D17), 1–17.

60 P. Formenti, W. Elbert, W. Maenhaut, J. Haywood and M. O. Andreae, Chemical composition of mineral dust aerosol during the Saharan Dust Experiment (SHADE) airborne campaign in the Cape Verde region, September 2000, *J. Geophys. Res.: Atmos.*, 2003, **108**(D18), 8576.

61 G. Young, H. M. Jones, E. Darbyshire, K. J. Baustian, J. B. McQuaid, K. N. Bower, *et al.*, Size-segregated compositional analysis of aerosol particles collected in the European Arctic during the ACCACIA campaign, *Atmos. Chem. Phys.*, 2016, **16**(6), 4063–4079.

62 C. L. Ryder, F. Marenco, J. K. Brooke, V. Estelles, R. Cotton, P. Formenti, *et al.*, Coarse-mode mineral dust size distributions, composition and optical properties from AER-D aircraft measurements over the tropical eastern Atlantic, *Atmos. Chem. Phys.*, 2018, **18**(23), 17225–17257.

63 A. Sanchez-Marroquin, D. H. P. Hedges, M. Hiscock, S. T. Parker, P. D. Rosenberg, J. Trembath, *et al.*, Characterisation of the filter inlet system on the FAAM BAe-146 research aircraft and its use for size-resolved aerosol composition measurements, *Atmos. Meas. Tech.*, 2019, **12**(11), 5741–5763.

64 M. S. C. Warner, Introduction to PySPLIT: A Python Toolkit for NOAA ARL's HYSPLIT Model, *Comput. Sci. Eng.*, 2018, **20**(5), 47–62.

65 T. F. Whale, B. J. Murray, D. O'Sullivan, T. W. Wilson, N. S. Umo, K. J. Baustian, *et al.*, A technique for quantifying heterogeneous ice nucleation in microlitre supercooled water droplets, *Atmos. Meas. Tech.*, 2015, **8**(6), 2437–2447.

66 D. A. Knopf, P. A. Alpert, A. Zipori, N. Reicher and Y. Rudich, Stochastic nucleation processes and substrate abundance explain time-dependent freezing in supercooled droplets, *npj Clim. Atmos. Sci.*, 2020, **3**(1), 1–9.

67 J. M. Creamean, R. M. Kirpes, K. A. Pratt, N. J. Spada, M. Maahn, G. de Boer, *et al.*, Marine and terrestrial influences on ice nucleating particles during continuous springtime measurements in an Arctic oilfield location, *Atmos. Chem. Phys.*, 2018, **18**(24), 18023–18042.

68 M. D. Petters and T. P. Wright, Revisiting ice nucleation from precipitation samples, *Geophys. Res. Lett.*, 2015, **42**(20), 8758–8766.

69 P. Israelevich, E. Ganor, P. Alpert, P. Kishcha and A. Stupp, Predominant transport paths of Saharan dust over the Mediterranean Sea to Europe, *J. Geophys. Res.: Atmos.*, 2012, **117**, 1–11.

70 C. S. Zender, R. L. R. L. Miller and I. Tegen, Quantifying mineral dust mass budgets: Terminology, constraints, and current estimates, *Trans., Am. Geophys. Union*, 2004, **85**(48), 509–512.

71 Y. Boose, A. Welti, J. D. Atkinson, F. Ramelli, A. Danielczok, H. G. Bingemer, *et al.*, Heterogeneous ice nucleation on dust particles sourced from nine deserts worldwide – Part 1: Immersion freezing, *Atmos. Chem. Phys.*, 2016, **16**(23), 15075–15095.

72 Y. Boose, B. Sierau, M. I. García, S. Rodríguez, A. Alastuey, C. Linke, *et al.*, Ice nucleating particles in the Saharan Air Layer, *Atmos. Chem. Phys.*, 2016, **16**(14), 9067–9087.

73 N. Reicher, L. Segev and Y. Rudich, The WeIzmann Supercooled Droplets Observation on a Microarray (WISDOM) and application for ambient dust, *Atmos. Meas. Tech.*, 2018, **11**(1), 233–248.

74 P. H. Gregory, Microbiology of the atmosphere, *Neth. J. Plant Pathol.*, 1973, **79**(6), 265.

75 V. R. Després, J. A. Huffman, S. M. Burrows, C. Hoose, A. S. Safatov, G. Buryak, *et al.*, Primary biological aerosol particles in the atmosphere: a review, *Tellus B*, 2012, **64**(1), 15598.

76 M. Nicolaisen, J. S. West, R. Sapkota, G. G. M. Canning, C. Schoen and A. F. Justesen, Fungal Communities Including Plant Pathogens in Near Surface Air Are Similar across Northwestern Europe, *Front. Microbiol.*, 2017, **8**, 1729.

77 E. Banchi, C. G. Ametrano, E. Tordoni, D. Stankovic, S. Ongaro, M. Tretiach, *et al.*, Environmental DNA assessment of airborne plant and fungal seasonal diversity, *Sci. Total Environ.*, 2020, **738**, 140249.

78 K. Wittmaack, H. Wehnes, U. Heinzmann and R. Agerer, An overview on bioaerosols viewed by scanning electron microscopy, *Sci. Total Environ.*, 2005, **346**(1–3), 244–255.

79 J. A. Huffman, B. Sinha, R. M. Garland, A. Snee-Pollmann, S. S. Gunthe, P. Artaxo, *et al.*, Size distributions and temporal variations of biological aerosol particles in the Amazon rainforest characterized by microscopy and real-time UV-APS fluorescence techniques during AMAZE-08, *Atmos. Chem. Phys.*, 2012, **12**(24), 11997–12019.

80 A. Kolpakova, J. Hovorka and M. Klán, Pollen Characterization in Size Segregated Atmospheric Aerosol, *IOP Conf. Ser. Earth Environ. Sci.*, 2017, **95**(6), 062001.

81 M. E. Lacey and J. S. West, *The Air Spora*, Springer US, 1st edn, 2006, vol. XVI, p. 156.

82 S. Matthias-Maser and R. Jaenicke, The size distribution of primary biological aerosol particles with radii > 0.2 μm in an urban/rural influenced region, *Atmos. Res.*, 1995, **39**(4), 279–286.

83 W. Li, L. Liu, L. Xu, J. Zhang, Q. Yuan, X. Ding, *et al.*, Overview of primary biological aerosol particles from a Chinese boreal forest: Insight into morphology, size, and mixing state at microscopic scale, *Sci. Total Environ.*, 2020, **719**, 137520.

84 R. Iannone, D. I. Chernoff, A. Pringle, S. T. Martin and A. K. Bertram, The ice nucleation ability of one of the most abundant types of fungal spores found in the atmosphere, *Atmos. Chem. Phys.*, 2011, **11**(3), 1191–1201.

85 A. T. Kunert, M. L. Pöhlker, K. Tang, C. S. Krevert, C. Wieder, K. R. Speth, *et al.*, Macromolecular fungal ice nuclei in Fusarium: effects of physical and chemical processing, *Biogeosciences*, 2019, **16**(23), 4647–4659.

86 I. Crawford, K. N. Bower, T. W. Choularton, C. Dearden, J. Crosier, C. Westbrook, *et al.*, Ice formation and development in aged, wintertime cumulus over the UK: observations and modelling, *Atmos. Chem. Phys.*, 2012, **12**(11), 4963–4985.

87 A. D. Harrison, K. Lever, A. Sanchez-Marroquin, M. A. Holden, T. F. Whale, M. D. Tarn, *et al.*, The ice-nucleating ability of quartz immersed in water and its atmospheric importance compared to K-feldspar, *Atmos. Chem. Phys. Discuss.*, 2019, **2019**, 1–23.